

(2)

AD-A235 286



Office of the Chief of Naval Research  
Contract N00014-87-K-0326  
Technical Report No. UWA/DME/TR-91/5

DYNAMIC FRACTURE RESPONSES OF  
 $\text{Al}_2\text{O}_3$ ,  $\text{Si}_3\text{N}_4$  AND  $\text{SiC}_w/\text{Al}_2\text{O}_3$

Y. Takagi and A.S. Kobayashi

April 1991

DTIC  
ELECTE  
APR 30 1991  
S E D

The research reported in this technical report was made possible through support extended to the Department of Mechanical Engineering, University of Washington, by the Office of Naval Research under Contract N00014-87-K-0326. Reproduction in whole or in part is permitted for any purpose of the United States Government.

DISTRIBUTION STATEMENT A

Approved for public release;  
Distribution Unlimited

DTIC FILE COPY

91 4 29 076



## DYNAMIC FRACTURE RESPONSES OF $\text{Al}_2\text{O}_3$ , $\text{Si}_3\text{N}_4$ AND $\text{SiC}_w/\text{Al}_2\text{O}_3$

Yoshio Takagi\* and Albert S. Kobayashi  
University of Washington  
Department of Mechanical Engineering  
Seattle, Washington 98195, USA

Accession For	
NTIS GRA&I <input checked="" type="checkbox"/>	
DTIC TAB <input type="checkbox"/>	
Unannounced <input type="checkbox"/>	
Justification	
By _____	
Distribution/ _____	
Availability Codes	
Dist	Avail and/or Special
A-1	

### ABSTRACT

A hybrid experimental-numerical procedure was used to characterize the dynamic fracture responses of alumina ( $\text{Al}_2\text{O}_3$ ), silicon nitride ( $\text{Si}_3\text{N}_4$ ) and silicon carbide whisker/alumina matrix ( $\text{SiC}_w/\text{Al}_2\text{O}_3$ ) composite. A laser interferometric displacement gage was used to determine through the crack opening displacement (COD), the instantaneous crack tip location during rapid fracture at room and 1000°C. Consistent with previous finding, the dynamic crack arrest stress intensity factor did not exist in the ceramics and ceramic matrix composite studied.

### INTRODUCTION

The projected use of ceramics and ceramic matrix composites in heat engines will subject these components to severe loading conditions, such as particulate impact at elevated temperature. While recent literature is abundant with data on impact studies of monolithic ceramics, similar research at elevated temperature is missing. From the user's viewpoint, impact studies provide practical failure data which relates directly to the functional capability of the ceramics and ceramic matrix composite components. These impact failures are characterized by shattering which is a complex phenomenon involving microcrack generation, growth and coalescence into macro-cracks which in turn grow, branch and coalesce.

A more generic analysis of impact failure is to study the dynamic crack initiation propagation and arrest stress intensity factors,  $K_{Id}$ ,  $K_I^{dyn}$  and  $K_{Ia}$ , respectively as well as crack branching in these brittle materials. While dynamic fracture mechanics has been the subject of active research for the past two decades, it has been exclusively confined to traditional metallic structure with polymers used as a model material in basic research. Similar dynamic fracture mechanics study of ceramics and ceramic matrix composites are virtually non-existent except for [1] in addition to those of the authors and their colleagues [2-10].

In the following, we report on the recent results generated through our continuing study on this subject.

\* On academic leave from NKK Corporation, Advanced Technology Research Center, Kawasaki 210, Japan.

## METHOD OF APPROACH

The hybrid experimental-numerical technique, which was developed by Yang et al [7] for dynamic fracture characterization of high temperature ceramics and ceramic composites, was used in this analysis with improved sensitivity. In the following a brief description of the procedure is provided.

### Material and specimen

Materials for the fracture specimen consists of commercially available alumina ( $\text{Al}_2\text{O}_3$ )\* silicon nitride ( $\text{Si}_3\text{N}_4$ )\*\* and a alumina matrix composite with 25% silicon carbide whisker ( $\text{SiC}_w/\text{Al}_2\text{O}_3$ )\*\*\*. The fracture specimens, which are single edge notched three point bend specimens, were machined to the dimensions shown in Figure 1. Three point bend specimens were used because of their simplicity in geometry and relative ease in alignment at elevated temperature. A shallow chevron notch was machined as a starter crack for initiating a true crack by the single-edge-precracked-beam (SEPB) method of [11]. These true crack were normally about 3-4 mm in depth.

### Experimental procedure

The loading system consisted of a drop weight tower, which is mounted integrally with the furnace which in turn can operate at a temperature up to 1500°C. The door and two port holes, which are shielded with fused silicate glass panes to prevent undesirable convection current of air in the furnace chamber, provided access for the input and output laser beams of the laser interferometric displacement gage (LIDG) [4,8]. The mass of the steel impactor was 2.2 kg. The specimens were rapidly loaded by the dropweight with an impact velocity of 0.7 m/sec. The impact load was monitored by a load transducer at the top end of a push rod and outside of the furnace as shown schematically in Figure 2.

A pair of LIDG targets were placed at the crack mouth of the specimen. The crack mouth opening displacement (CMOD) obtained from the LIDG records was used to determine directly the crack tip location in a rapidly fracturing three point bend specimen. The LIDG targets were platinum tabs which were mounted directly on the specimen after precracking and then indented by a Vickers microhardness tester to minimize possible experimental error in locating the LIDG targets.

A series of static tests were also conducted at room temperature in order to obtain dynamic fracture data at low crack velocity. This data was necessary to highlight the significant differences between the dynamic fracture responses of metals and brittle ceramics and ceramic composites at  $K_I^{\text{dyn}}$  substantially lower than the static fracture toughness,  $K_{IC}$ .

### Numerical procedure

The crack tip location versus time history together with the loading history were used to execute a dynamic finite element code in its generation mode in order to compute the dynamic initiation and the propagation stress intensity factors,  $K_{Id}$  and  $K_I^{\text{dyn}}$ , respectively, associated with the propagating crack. Details of this hybrid experimental-numerical procedure as well as its validation are given in [7,8].

---

\* AD-995 Coors Porcelain Company, Golden, Colorado 80401  
\*\* NKK Corporation, Kawasaki 210, Japan  
\*\*\* A30SC Nippon Steel Corporation, Kawasaki 211, Japan.

## RESULTS

The above mentioned procedure was used to generate the dynamic stress intensity factor,  $K_I^{dyn}$ , versus crack velocity relations for  $\text{Al}_2\text{O}_3$ ,  $\text{Si}_3\text{N}_4$  and  $\text{SiC}_w/\text{Al}_2\text{O}_3$  composite at room temperature and 1000°C. Figure 3 shows a pair of typical LIDG data together with the loading history obtained for the  $\text{SiC}_w/\text{Al}_2\text{O}_3$  specimen tested at 1000°C. Figure 4 shows the resultant crack extension history obtained by this LIDG data at the crack mouth. Figure 5 shows the CMOD and the crack extension histories for the  $\text{Si}_3\text{N}_4$  specimens tested at room temperature.

As mentioned previously, the crack extension and load histories were then used to compute the dynamic initiation and propagation stress intensity factors,  $K_{Id}$  and  $K_I^{dyn}$ , respectively, the results of which are reported in the following.

### Dynamic fracture initiation toughness, $K_{Id}$

Since the initial cracks generated by the SEPB method is a true crack, the dynamic initiation stress intensity factor,  $K_{Id}$ , obtained in this study should be less than those reported previously [8-10]. Table 1 shows a tabulated comparison of these  $K_{Id}$  where  $K_{Id}$  in this study is slightly higher than those of [10], but is within the expected scatter band of  $\pm 10\%$ . The high  $K_{Id}$  and  $K_{IC}$  for  $\text{Si}_3\text{N}_4$  are attributed to acicular  $\text{Si}_3\text{N}_4$ , which acts as whiskers in the crystalline  $\text{Si}_3\text{N}_4$  matrix.

Table 1 Comparison of fracture toughnesses

Ref.	Fracture Toughness (MPa $\sqrt{\text{m}}$ )	Alumina		Silicon Nitride		$\text{SiC}_w/\text{Al}_2\text{O}_3$ Composite	
		Temp.		Temp.		Temp.	
		Room	1000°C	Room	1000°C	Room	1000°C
This study	$K_{Id}$ $K_{IC}$	4.9 -	4.4 -	9.9 9.0	- -	5.6 6.0	5.9 -
Yang and Kobayashi (1990)	$K_{Id}$ $K_{IC}$	5.7 4.3	5.1 -			7.9 6.6	6.9 -
Duffy et al. (1988)	$K_{Id}$ $K_{IC}$	5.6 3.4	- -				

### Dynamic stress intensity factor, $K_I^{dyn}$ and arrest

Figures 6, 7 and 8 show the dynamic stress intensity factor (SIF),  $K_I^{dyn}$  versus crack velocity relations for  $\text{Al}_2\text{O}_3$ ,  $\text{Si}_3\text{N}_4$  and  $\text{SiC}_w/\text{Al}_2\text{O}_3$  composite, respectively. Data points for the lower dynamic stress intensity factors and lower crack velocities were obtained through statically loaded specimens. These results show an unambiguous lack of dynamic crack arrest stress intensity factor below which dynamic crack propagation will cease. The crack velocities for impacted specimens in this study were on the average about four

times of that of [10] for identical alumina fracture specimens. It was about twenty percent higher for the different  $\text{SiC}_w/\text{Al}_2\text{O}_3$  specimens used in this study.

Figures 7 and 8 show that the crack can propagate at a larger crack velocity under high  $K_I^{dyn}$ . Therefore no unique crack velocity versus  $K_I^{dyn}$  can be observed in these materials.

## CONCLUSIONS

The hybrid experimental-numerical procedure was used to determine the crack velocity versus dynamic stress intensity factor relations in  $\text{Al}_2\text{O}_3$ ,  $\text{Si}_3\text{N}_4$  and  $\text{SiC}_w/\text{Al}_2\text{O}_3$  composite at room temperature and 1000°C. The results, which are in qualitative agreement with [2-10], again showed conclusively the lack of a dynamic crack arrest intensity factor and of a unique crack velocity versus dynamic stress intensity factor relation.

## DISCUSSIONS

The fracture surfaces were scanned by SEM and the relative areas of transgranular failures of the silicon nitride grains and the alumina grains in the statically loaded and impact loaded  $\text{Si}_3\text{N}_4$  and  $\text{SiC}_w/\text{Al}_2\text{O}_3$  composite were compared.

Figures 9 and 10 show typical fracture surfaces of a dynamically and a statically loaded  $\text{Si}_3\text{N}_4$  and  $\text{SiC}_w/\text{Al}_2\text{O}_3$  specimens at room temperature. Transgranular fracture dominated the fracture in the statically loaded specimen while the dynamically loaded specimen is characterized by the predominant intergranular fracture.

Figure 11 shows the percentage area of transgranular fracture versus dynamic SIF relation for  $\text{SiC}_w/\text{Al}_2\text{O}_3$  specimens. The percentage area of transgranular fracture is in excess of 45% at the lowest SIF of about  $1 \text{ MPa}\sqrt{\text{m}}$ . These results are consistent with those of Figure 8 thus suggesting a correlation between the percentage area of transgranular fracture and the crack velocity which is shown in Figure 12. The percentage area of transgranular fracture increases almost linearly with the crack velocity in this figure. The percentage area of transgranular is more than 40% even with the low crack velocity of 40 m/s. The kinematic constraint of a rapidly propagating crack probably enforces transgranular fracture which in turn enables the crack to propagate at a subcritical dynamic SIF. The lack of crack arrest of the propagating crack in this study was thus attributed to the large percentage area of transgranular failures in contrast to that of the arrested precrack tip region discussed previously [10,14].

## ACKNOWLEDGEMENT

This research was supported by Office of Naval Research Contract No. N00014-87-K-0326. The authors wish to thank Drs. Yapa Rajapakse and Steve Fishman, ONR for their patience and support. The authors are specially indebted to Mr. Tetsuo Nose, Nippon Steel Corporation for providing the SEPB fixture and the  $\text{SiC}_w/\text{Al}_2\text{O}_3$  specimens for this study and to NKK Corporation for providing the  $\text{Si}_3\text{N}_4$  specimens.

## REFERENCES

1. Gonczy, S.T. and Johnson, D.L., "Impact Fracture of Ceramics at High Temperatures," Fracture Mechanics of Ceramics, vol. 3, R.C.Bradt, D.P.H. Hasselman and F.F. Lange (eds) Plenum Press, pp. 495-506 (1978).
2. Kobayashi, A.S., Emery, A.F. and Liaw, B.M., "Dynamic Toughness of Glass," Fracture Mechanics of Ceramics, Vol. 6 eds R.C. Bradt, A.G. Evans, D.P.H. Hasselman and F.F. Lange, Plenum Press, pp 47-62 (1983).
4. Kobayashi, A.S. and Yang, K.-H., "A Hybrid Technique for High-Temperature Dynamic Fracture Analysis," Applications of Advanced Measurement Techniques, Brit. Soc for Strain Measurements, Whittles Pub., Caithness, U.K., pp. 109-120 (1988).
5. Kobayashi, A.S., Yang, K.-H. and Emery, A.F., "Dynamic Fracture Testing of Alumina," Impact Loading and Dynamic Behavior of Materials, C.Y. Chiem, H.-D. Kunze and L.W. Meyer (eds.) DGB Informationsgesellschaft mgH, pp. 113-119 (1988).
6. Liaw, B.M., Kobayashi, A.S., and Emery, A.F., "Effect of Loading Rates on Dynamic Fracture of Reaction Bonded Silicon Nitride," Fracture Mechanics: Seventh Volume, ASTM STP 905, pp.95-107 (1986).
7. Yang, Kwan-Ho and Kobayashi, Albert S., "An Experimental-Numerical Procedure for High Temperature Dynamic Fracture Analysis," Computational Mechanics '88, ed. S.N. Atluri and G. Yagawa, Springer-Velag, pp. 48v.1-48v.4 (1988).
8. Yang, K.-H., Kobayashi, A.S. and Emery, A.F., "Dynamic Fracture Characterization of Ceramic Matrix Composites," Journal de Physique, Colloque C3, supplément au No. 9, C3-223-230 (1988).
9. Yang, K.-H., Kobayashi, A.S. and Emery, A.F., "Effects of Loading Rates and Temperature on Dynamic Fracture of Ceramics and Ceramic Matrix Composites," Ceramic Materials and Components for Engines, V.J. Tennery and M.K. Ferber, American Ceramic Society (eds.), pp. 766-775 (1989).
10. Yang, K.-H. and Kobayashi, A.S., 1990, "Dynamic Fracture Response of Alumina and Two Ceramic Composites." Journal of American Ceramic Society, 73 (8), pp. 2309-2315 (1990).
11. Nose, T. and Fujii, T., "Evaluation of Fracture Toughness for Ceramic Materials by a Single-Edge-Precracked-Beam Method," Journal of the American Ceramic Society, Vol. 71, No.6, pp. 328-333 (1988).
12. Duffy, J., Suresh, S., Cho, K. and Bopp, E.R., "A Method for Dynamic Fracture Initiation Testing of Ceramics," Journal of Engineering Materials and Technology, Vol 110, No. 4, pp. 325-31(1988).
13. Yu, C.-T. and Kobayashi, A.S., "Fracture Process Zone in Ceramics and Ceramic Composites," to be published in Proc. of 6th Int'l Conf. on Mechanical Behavior of Materials, Kyoto, Japan, July 1991.
14. Yang, W.-J, Yu, C.T. and Kobayashi, A.S., "SEM Quantification of Trans- versus Inter-granular Fracture," to be published in J. of Am. Ceramic Soc.

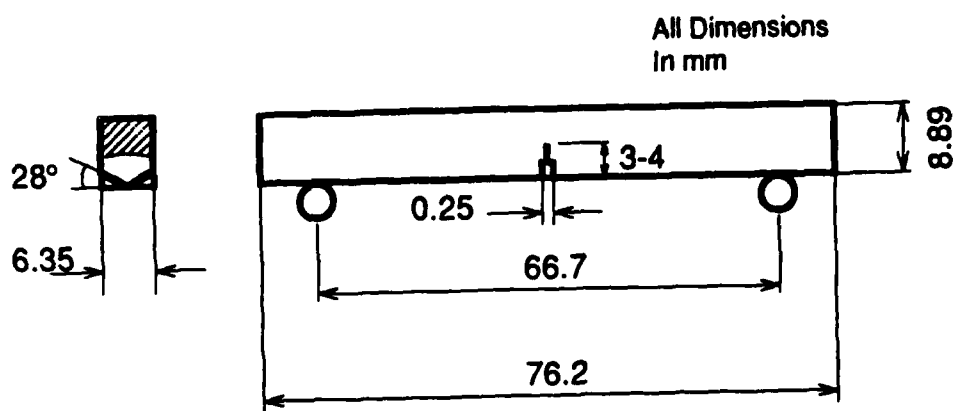


Figure 1. Precracked Three-point Bend Speciem.

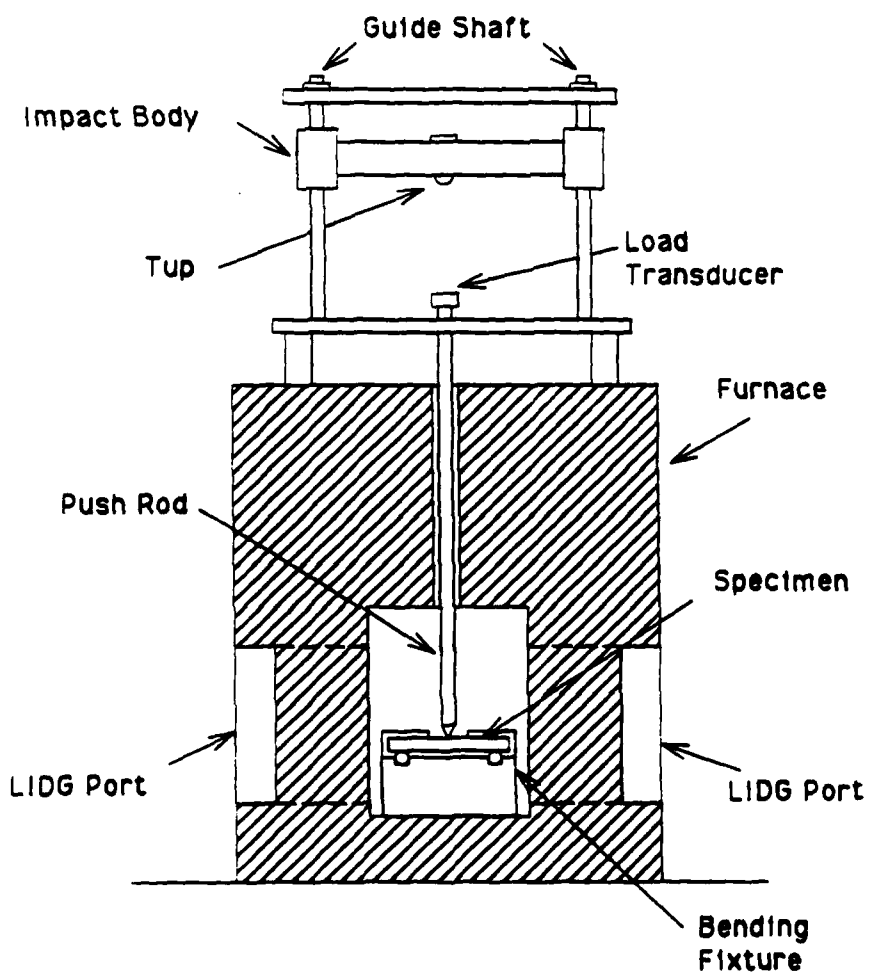


Figure 2. Drop-weight Impact Tester and Furnace with LIDG Ports.

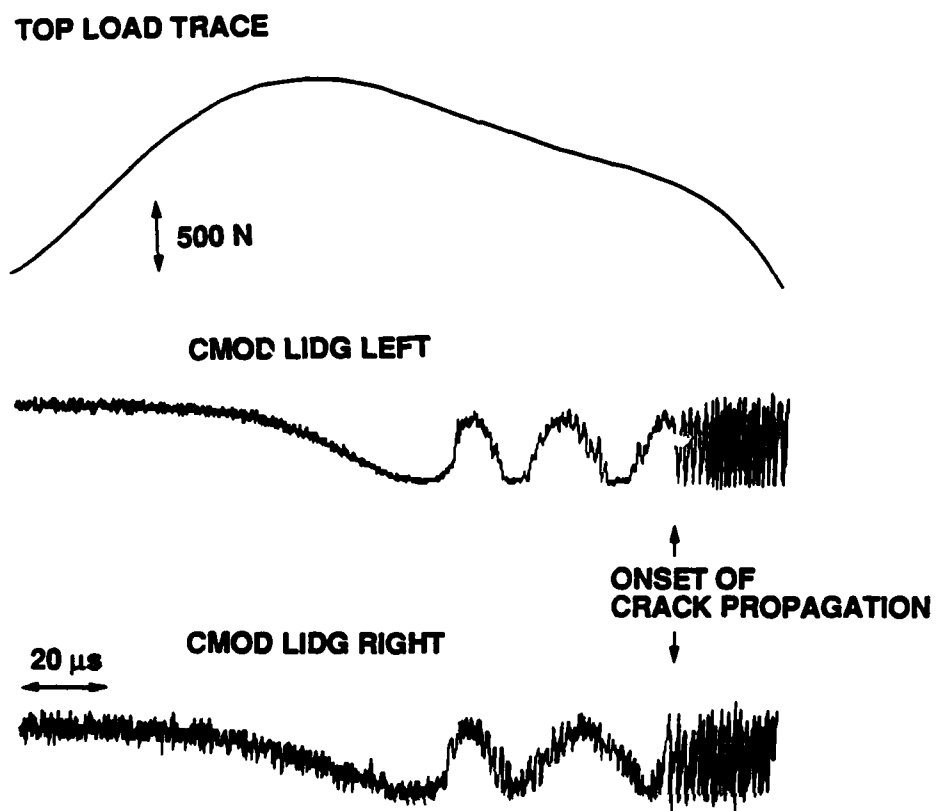


Figure 3. Loading and CMOD Histories at 1000°C.  $\text{SiC}_w/\text{Al}_2\text{O}_3$  Specimen.

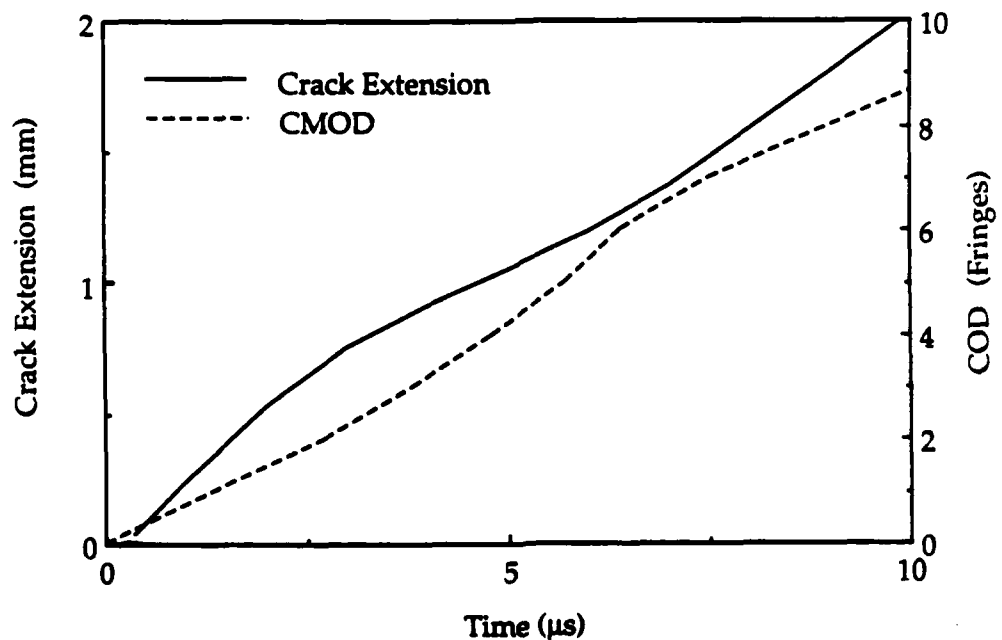


Figure 4. CMOD and Crack Extension Histories at 1000°C.  $\text{SiC}_w/\text{Al}_2\text{O}_3$  Specimen.

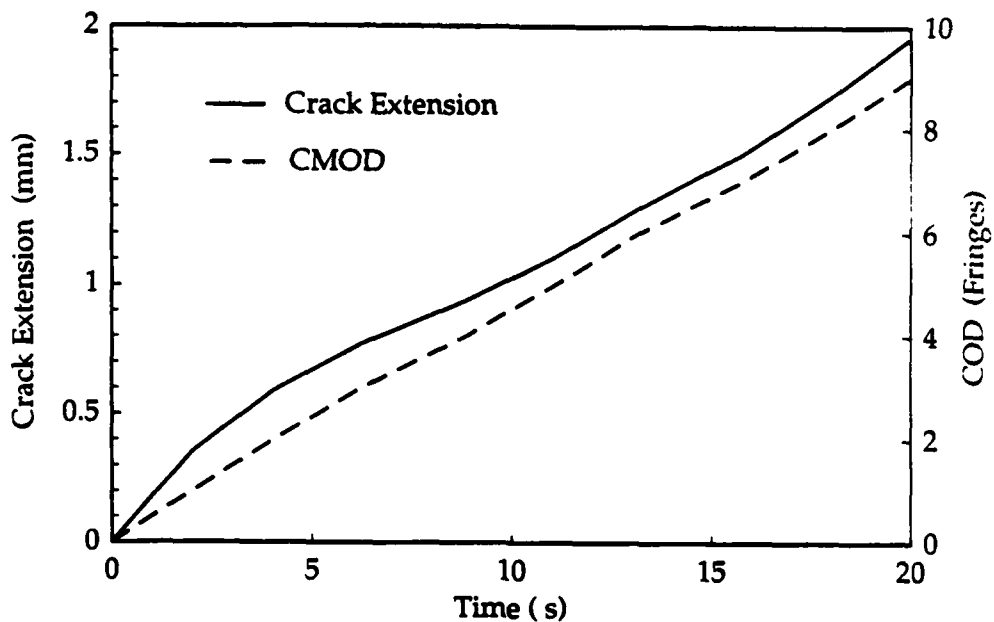


Figure 5. COD and Crack Extension Histories at Room Temperature.  $\text{Si}_3\text{N}_4$  Specimen.

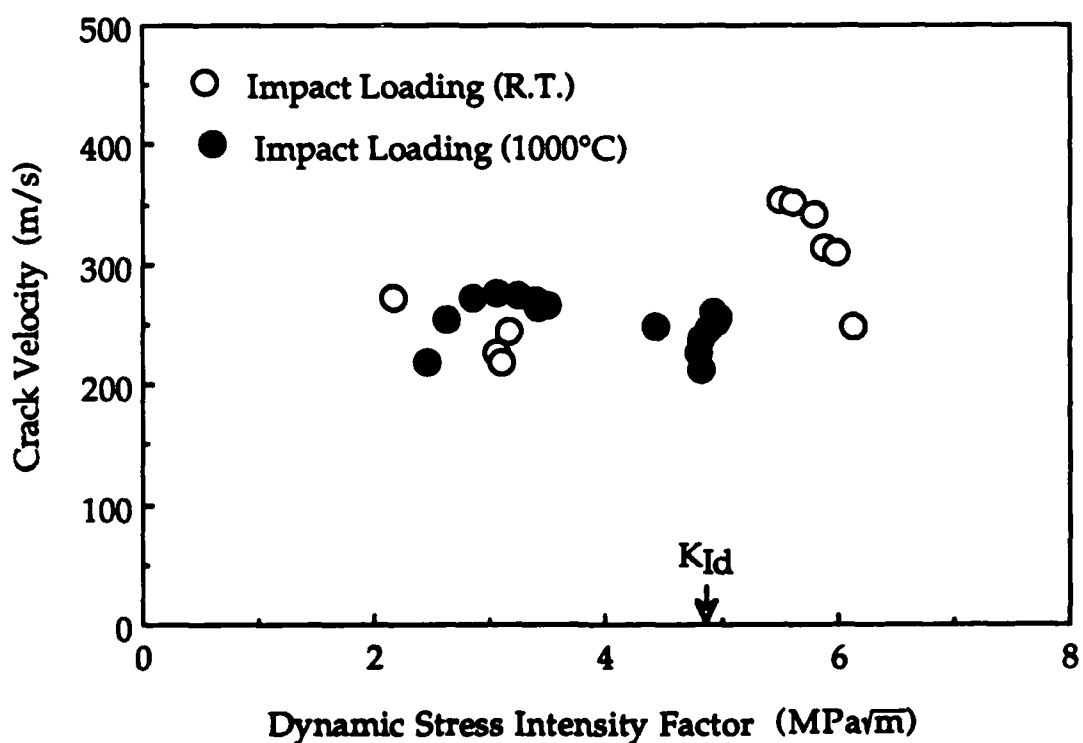


Figure 6. Dynamic SIF versus Crack Velocity Relation of  $\text{Al}_2\text{O}_3$ .

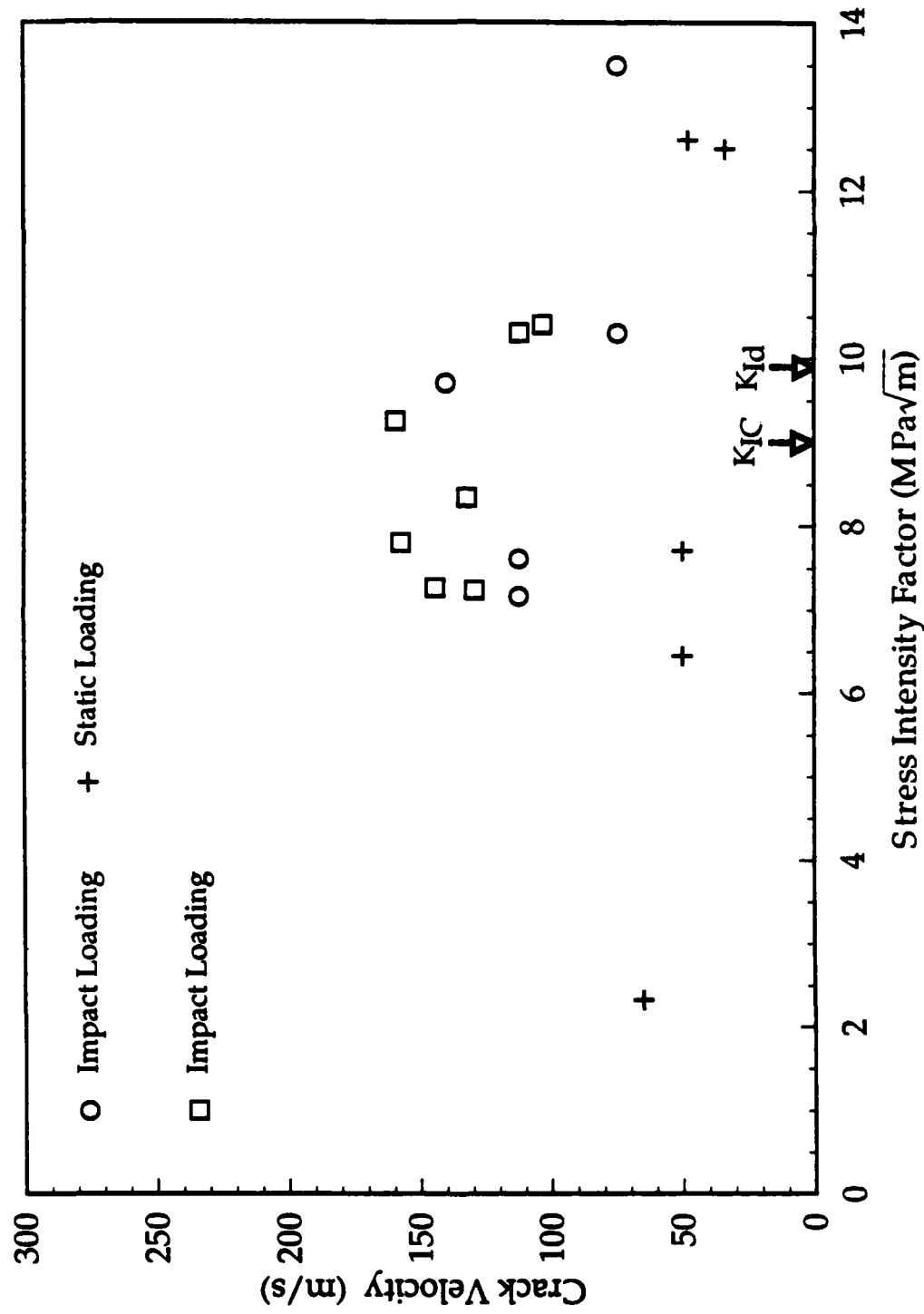


Figure 7. Stress Intensity Factor versus Crack Velocity of  $\text{Si}_3\text{N}_4$  at Room Temperature.

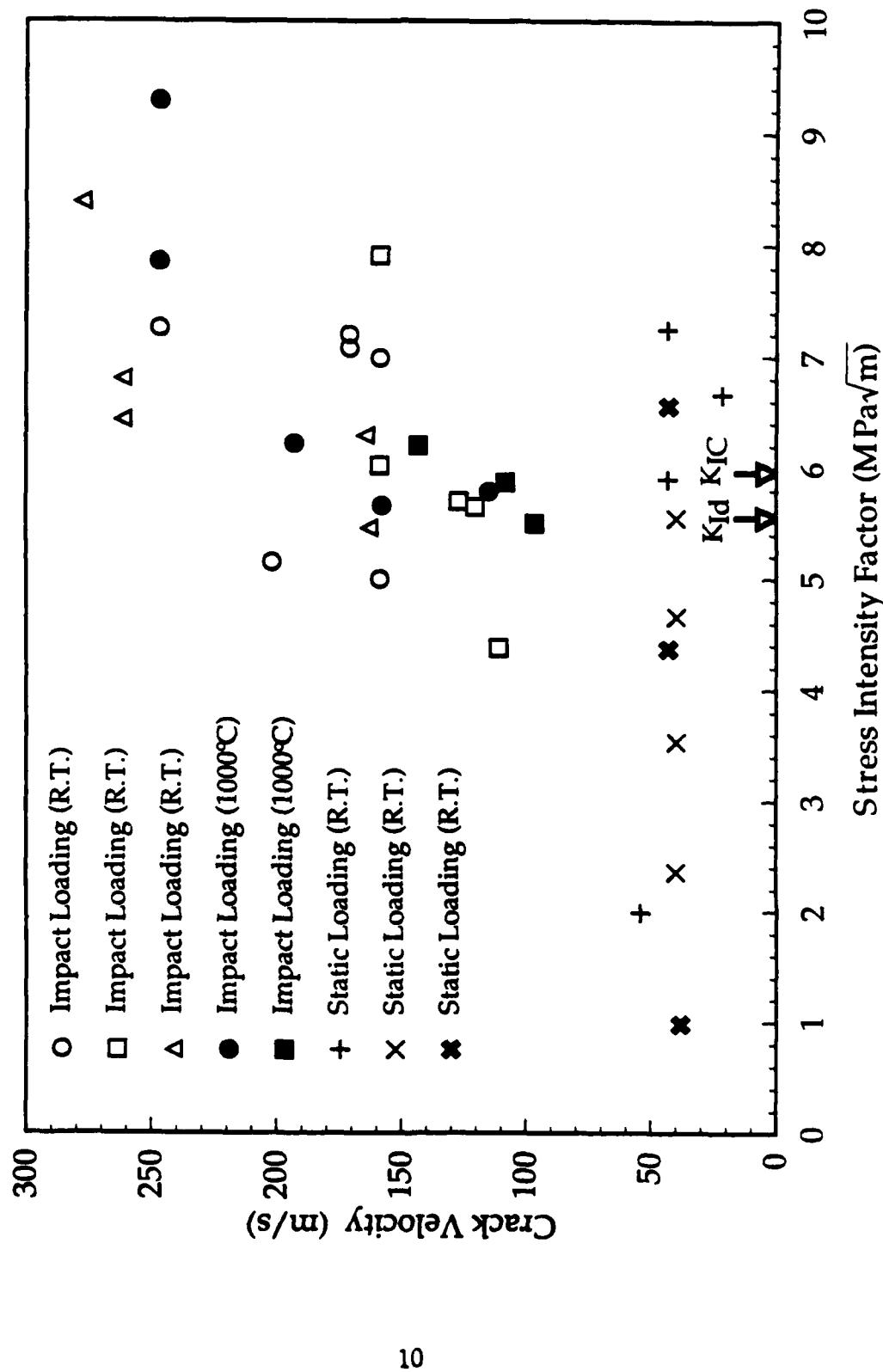
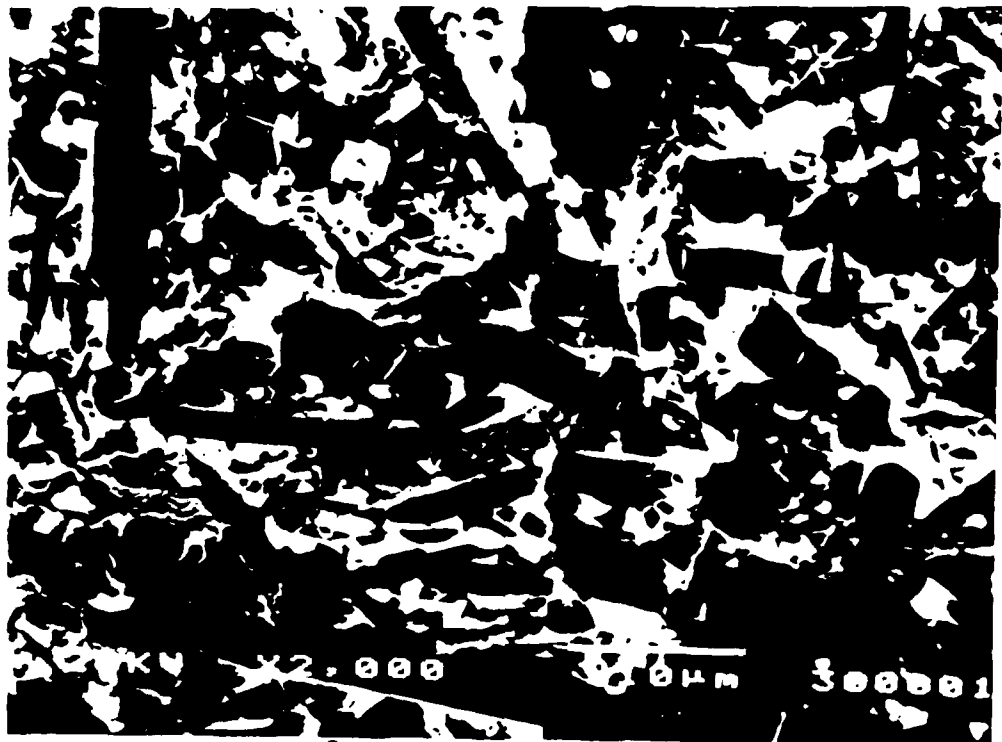


Figure 8. Stress Intensity Factor versus Crack Velocity of SiC<sub>w</sub>/Al<sub>2</sub>O<sub>3</sub>.

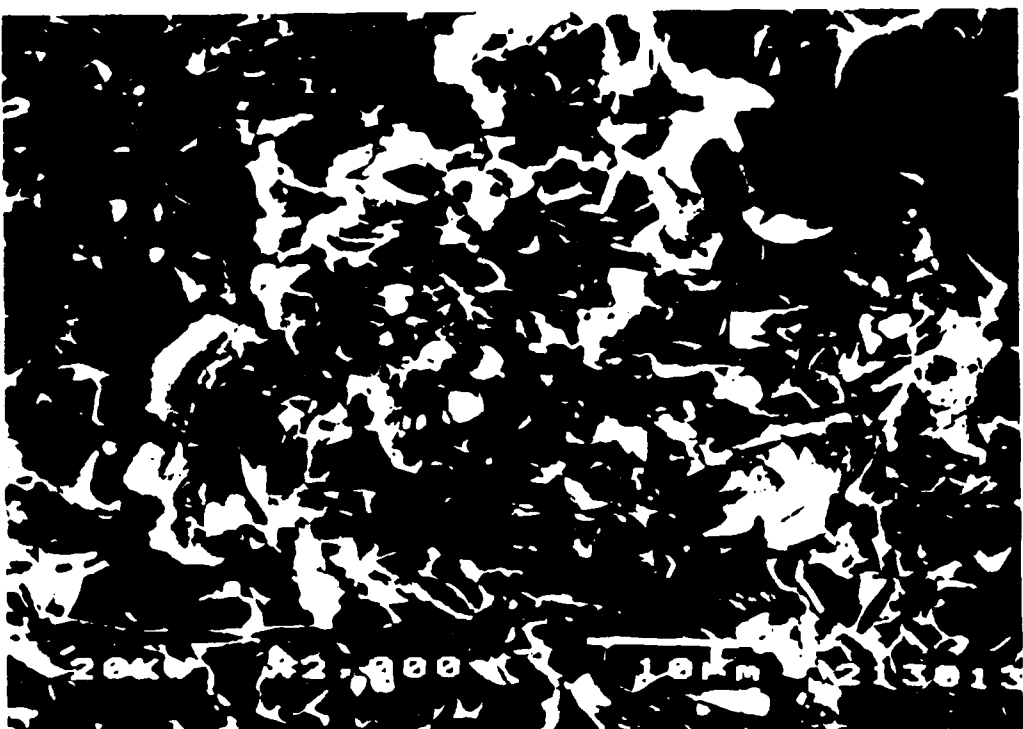


Statically Loaded Specimen

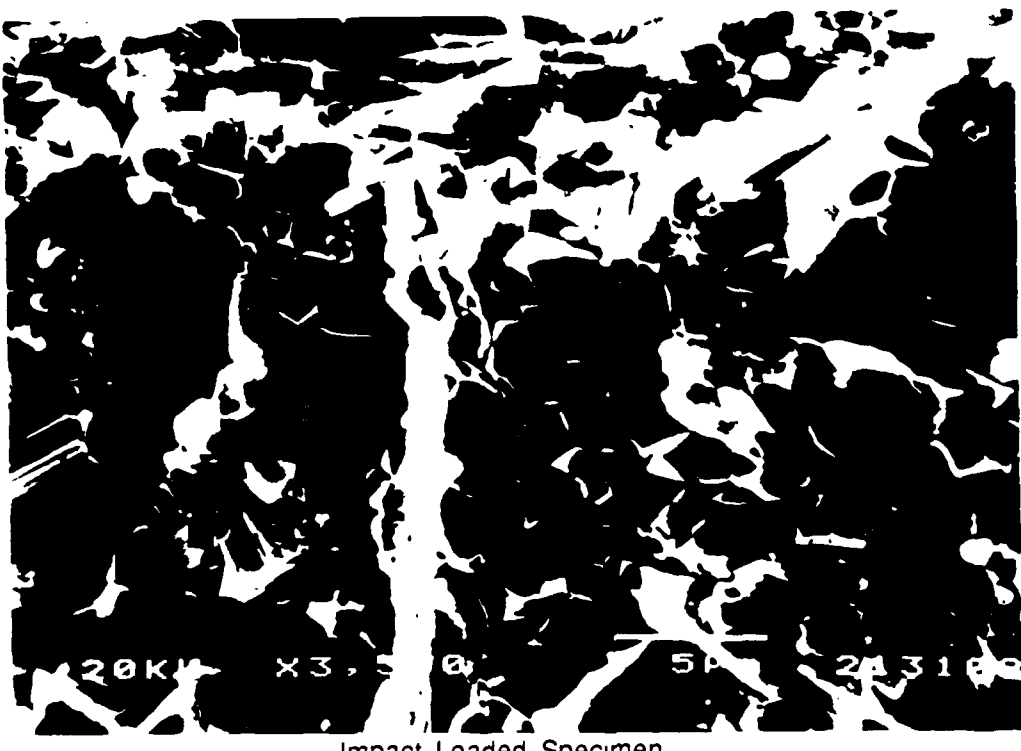


Impact Loaded Specimen

Figure 9. Fracture Surfaces of Si<sub>3</sub>N<sub>4</sub> Specimens Tested at Room Temperature.



Statically Loaded Specimen



Impact Loaded Specimen

Figure 10. Fracture Surfaces of SiC<sub>w</sub>/Al<sub>2</sub>O<sub>3</sub> Specimens Tested at Room Temperature.

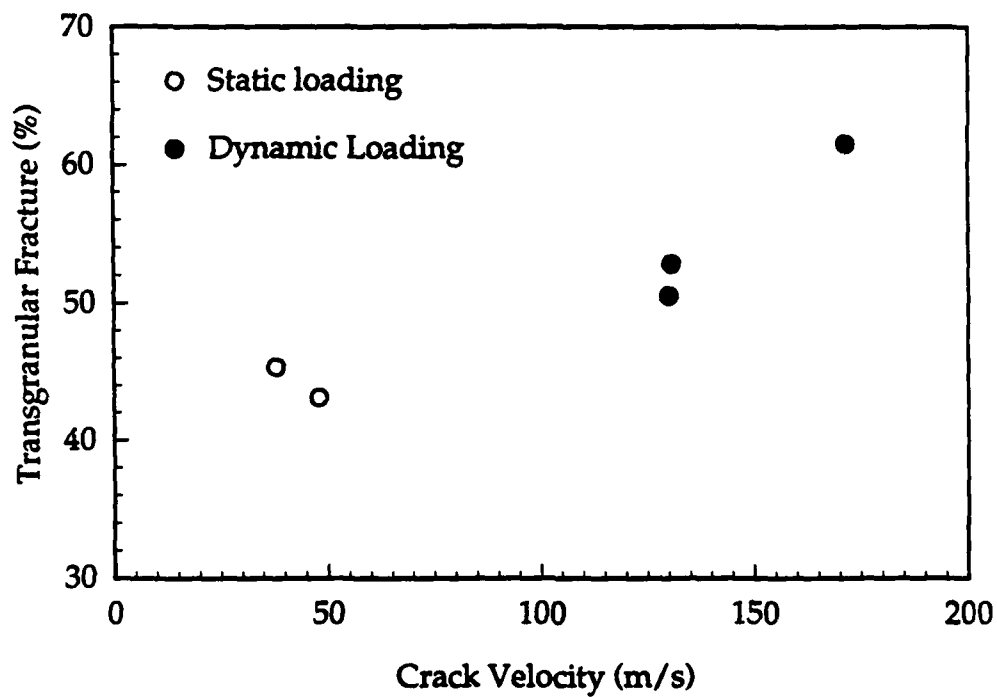


Figure 11. Percentage Area of Transgranular Fracture versus Stress Intensity Factor.  $\text{SiC}_w/\text{Al}_2\text{O}_3$  Specimens.

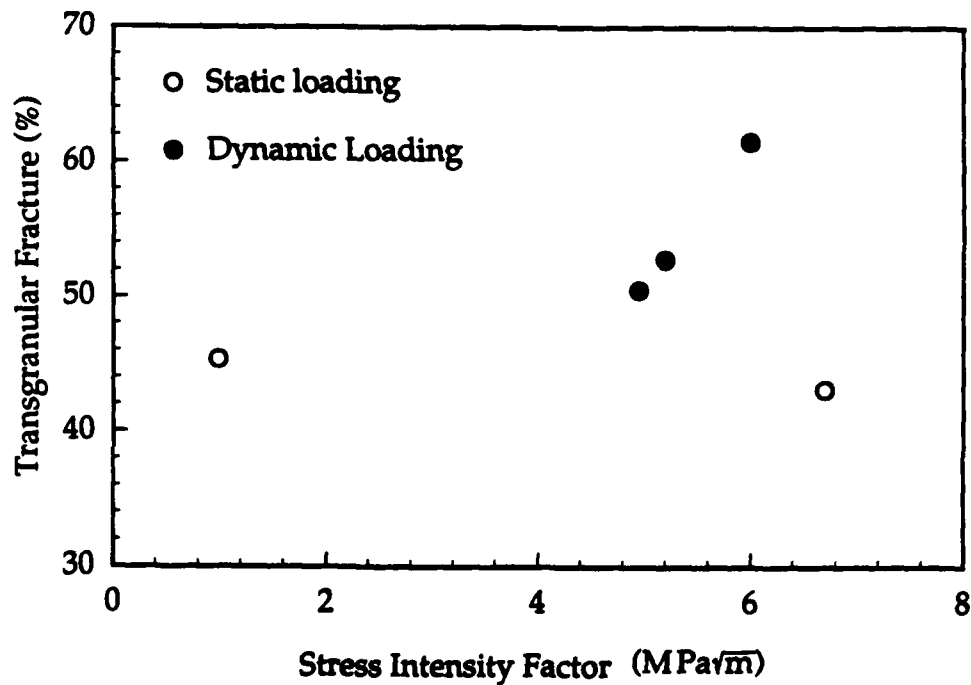


Figure 12. Percentage Area of Transgranular Fracture versus Crack Velocity.  $\text{SiC}_w/\text{Al}_2\text{O}_3$  Specimens.

UNCLASSIFIED

SECURITY CLASSIFICATION OF THIS PAGE

Form Approved  
OMB No. 0704-0188

## REPORT DOCUMENTATION PAGE

1a. REPORT SECURITY CLASSIFICATION Unclassified		1b. RESTRICTIVE MARKINGS	
2a. SECURITY CLASSIFICATION AUTHORITY		3. DISTRIBUTION/AVAILABILITY OF REPORT Unlimited	
2b. DECLASSIFICATION/DOWNGRADING SCHEDULE			
4. PERFORMING ORGANIZATION REPORT NUMBER(S) UWA/DME/TR-91/5		5. MONITORING ORGANIZATION REPORT NUMBER(S)	
6a. NAME OF PERFORMING ORGANIZATION University of Washington	6b. OFFICE SYMBOL (if applicable)	7a. NAME OF MONITORING ORGANIZATION	
6c. ADDRESS (City, State, and ZIP Code) Department of Mechanical Engineering, FU-10 Seattle, WA 98195		7b. ADDRESS (City, State, and ZIP Code)	
8a. NAME OF FUNDING/SPONSORING ORGANIZATION Office of Naval Research	8b. OFFICE SYMBOL (if applicable) ONR	9. PROCUREMENT INSTRUMENT IDENTIFICATION NUMBER S40050srh03: Dated 21 Dec. 1988	
9c. ADDRESS (City, State, and ZIP Code) Arlington, VA 22217-5000		10. SOURCE OF FUNDING NUMBERS	
		PROGRAM ELEMENT NO. N00014	PROJECT NO. 37-K-0326
		TASK NO.	WORK UNIT ACCESSION NO.
11. TITLE (Include Security Classification) Dynamic Fracture Responses of Al <sub>2</sub> O <sub>3</sub> , Si <sub>3</sub> N <sub>4</sub> and SiC <sub>w</sub> /Al <sub>2</sub> O <sub>3</sub>			
12. PERSONAL AUTHOR(S) Y. Takagi and A.S. Kobayashi		13. TYPE OF REPORT Technical Report	
13b. TIME COVERED FROM Aug. 89. to Mar 91		14. DATE OF REPORT (Year, Month, Day) 1991 April 4	
15. PAGE COUNT 13			
16. SUPPLEMENTARY NOTATION			
17. COSATI CODES		18. SUBJECT TERMS (Continue on reverse if necessary and identify by block number)	
FIELD	GROUP	SUB-GROUP	

## 19. ABSTRACT (Continue on reverse if necessary and identify by block number)

A hybrid experimental-numerical procedure was used to characterize the dynamic fracture responses of alumina (Al<sub>2</sub>O<sub>3</sub>), silicon nitride (Si<sub>3</sub>N<sub>4</sub>) and silicon carbide whisker/alumina matrix (SiC<sub>w</sub>/Al<sub>2</sub>O<sub>3</sub>) composite. A laser interferometric displacement gage was used to determine through the crack opening displacement (COD), the instantaneous crack tip location during rapid fracture at room and 1000°C. Consistent with previous finding, the dynamic crack arrest stress intensity factor did not exist in the ceramics and ceramic matrix composite studied.

20. DISTRIBUTION/AVAILABILITY OF ABSTRACT <input checked="" type="checkbox"/> UNCLASSIFIED/UNLIMITED <input type="checkbox"/> SAME AS RPT. <input type="checkbox"/> DTIC USERS	21. ABSTRACT SECURITY CLASSIFICATION Unclassified
22a. NAME OF RESPONSIBLE INDIVIDUAL A.S. Kobayashi	22b. TELEPHONE (include Area Code) (206)543-5488
22c. OFFICE SYMBOL	